Journal of Ultrafine Grained and Nanostructured Materials
Vol.48, No.2, December 2015, pp.113-124
https://jufgnsm.ut.ac.ir
Print ISSN: 2423-6845 Online ISSN: 2423-6837
DOI: 10.7508/jufgnsm.2015.02.006

Exact solution for the vibrations of cylindrical nanoshells considering surface energy effect

Hessam Rouhi, Reza Ansari*, Mansour Darvizeh

Department of Mechanical Engineering, University of Guilan, P.O. Box 3756, Rasht, Iran

Received 8 October 2015; Accepted 6 December 2015
* *Corresponding Author Email: r_ansari@guilan.ac.ir, Tel. /fax: +98 13 33690276*

Abstract
It has been revealed that the surface stress effect plays an important role in the mechanical behavior of structures (such as bending, buckling and vibration) when their dimensions are on the order of nanometer. In addition, recent advances in nanotechnology have proposed several applications for nanoscale shells in different fields. Hence, in the present article, within the framework of surface elasticity theory, the free vibration behavior of simply-supported cylindrical nanoshells with the consideration of the aforementioned effect is studied using an exact solution method. To this end, first, the governing equations of motion and boundary conditions are obtained by an energy-based approach. The surface stress influence is incorporated into the formulation according to the Gurtin-Murdoch theory. The nanoshell is modeled according to the first-order shear deformation shell theory. After that, the free vibration problem is solved through an exact solution approach. To this end, the dimensionless form of governing equations is derived and then solved under the simply-supported boundary conditions using a Navier-type solution method. Selected numerical results are presented about the effects of surface stress and surface material properties on the natural frequencies of nanoshells with different radii and lengths. The results show that the surface energies significantly affect the vibrational behavior of nanoshells with small magnitudes of thickness. Also, it is indicated that the natural frequency of the nanoshell is dependent of the surface material properties.

Keywords: *exact method, nanoshell, natural frequency, surface effect.*

1. Introduction

Nanoscale structures have many applications in several cases such as composites [1, 2], sensors [3, 4], clinical applications [5], and solar cells [6]. A primary reason for the considerable interest in using nanostructures is related to their outstanding properties [7-10]. Nanoshells have recently attracted the attention of researchers for numerous applications [11-13].

The theoretical models based on the continuum mechanics are widely used so as to study the mechanical behavior of structures at micro- and nanoscale [14-17]. It is generally accepted that the use of the continuum models on the basis of classical elasticity theory does not lead to accurate results at very small

scales. Thus, some modified elasticity theories have been developed to capture the small scale effects on the mechanical behavior of micro- and nanostructures. Among them, the strain gradient theory [18-20], the nonlocal theory [21-23], and the couple stress theory [24-26] can be mentioned.

Also, an important issue in investigating the mechanical behavior of micro- and nanostructures is the heterogeneity nature of the material structure [27-29]. These structures are made of nano-structured materials including nano-porous materials, nanoparticle composites, and nanocrystalline materials [27-29]. Experimental and theoretical studies on the mechanics of nano-structured materials have revealed that they have unique properties that distinguish them from conventional materials. The ultra-small inhomogeneity sizes and the ultra-high specific interface areas can be mentioned as those properties [30].

The surface stress effect is a significant small size parameter that plays an important role in the mechanical response of nanostructures. In a nanostructure, due to dissimilar environmental conditions, atoms at or near a free surface have different equilibrium requirements as compared to the atoms within the bulk of material. This leads to the creation of surface stresses which become considerable as compared to their bulk counterparts when the size is very small. In 1970s, Gurtin and Murdoch [31, 32] proposed a modified elasticity theory called the surface elasticity theory in order to consider the surface stress effect in the continuum modeling of materials. Based on this theory, the physical properties in the neighborhood of surface are different from those of interior. Up to now, several researchers have successfully employed the Gurtin-Murdoch theory for the linear static [33-35], linear dynamic [36, 37], nonlinear static [38], and nonlinear dynamic [39-41] analyses of different nanostructures.

The literature review reveals that the majority of studies about the surface stress effect are related to the mechanical behavior of nanowires, nanobeams, and nanoplates; and the mechanical response of nanoshells incorporating surface stress effect has rarely been investigated so far. In the present research, based on the Gurtin-Murdoch theory capturing the surface stress effect, a continuum shell model is developed in order to investigate the vibrations of circular cylindrical nanoshells. To accomplish this aim, using the first-order shear deformation shell theory and Hamilton's principle, the governing equations of motion including surface influences are derived. Then, an exact solution is obtained for the free vibrations of nanoshells under simply-supported boundary conditions. In the numerical results, the surface stress effect and the influences of surface material properties are studied. The results of present work can pave the way for further investigations on the mechanical behavior of nanoshells considering surface effects within a reliable mathematical framework.

2. Derivation of Governing Equations

Consider a simply-supported cylindrical nanoshell with length L, thickness h and mid-surface radius R according to Figure 1. Based on the surface elasticity theory, a bulk part and two inner and outer thin surface layers are assumed for the nanoshell. A coordinate system is chosen whose origin is located on the middle surface of nanoshell. In this system, the longitudinal, circumferential, and transvers directions are respectively denoted by x, y and z. Using the first-order shear deformation shell theory, the displacement components are given as:

$$\begin{aligned} u_x(t,x,y,z) &= u(t,x,y) + z\psi_x(t,x,y), \\ u_y(t,x,y,z) &= v(t,x,y) + z\psi_y(t,x,y), \\ u_z(t,x,y,z) &= w(t,x,y). \end{aligned} \tag{1}$$

where t denotes the time. Also, u, v and w are the displacements of middle surface; ψ_x, and ψ_y are the rotations of the middle surface normals about the y- and x- axis, respectively.

The strain-displacement relations are expressed as:

$$\begin{Bmatrix} \varepsilon_{xx} \\ \varepsilon_{yy} \\ \gamma_{xy} \end{Bmatrix} = \begin{Bmatrix} \varepsilon_{xx}^{0} \\ \varepsilon_{yy}^{0} \\ \gamma_{xy}^{0} \end{Bmatrix} + z \begin{Bmatrix} \kappa_{xx} \\ \kappa_{yy} \\ \kappa_{xy} \end{Bmatrix} = \begin{Bmatrix} \dfrac{\partial u}{\partial x} \\ \dfrac{\partial v}{\partial y} + \dfrac{w}{R} \\ \dfrac{\partial u}{\partial y} + \dfrac{\partial v}{\partial x} \end{Bmatrix} + z \begin{Bmatrix} \dfrac{\partial \psi_x}{\partial x} \\ \dfrac{\partial \psi_y}{\partial y} \\ \dfrac{\partial \psi_x}{\partial y} + \dfrac{\partial \psi_y}{\partial x} \end{Bmatrix}, \begin{Bmatrix} \gamma_{xz} \\ \gamma_{yz} \end{Bmatrix} = \begin{Bmatrix} \psi_x + \dfrac{\partial w}{\partial x} \\ \psi_y + \dfrac{\partial w}{\partial y} - \dfrac{v}{R} \end{Bmatrix} \tag{2}$$

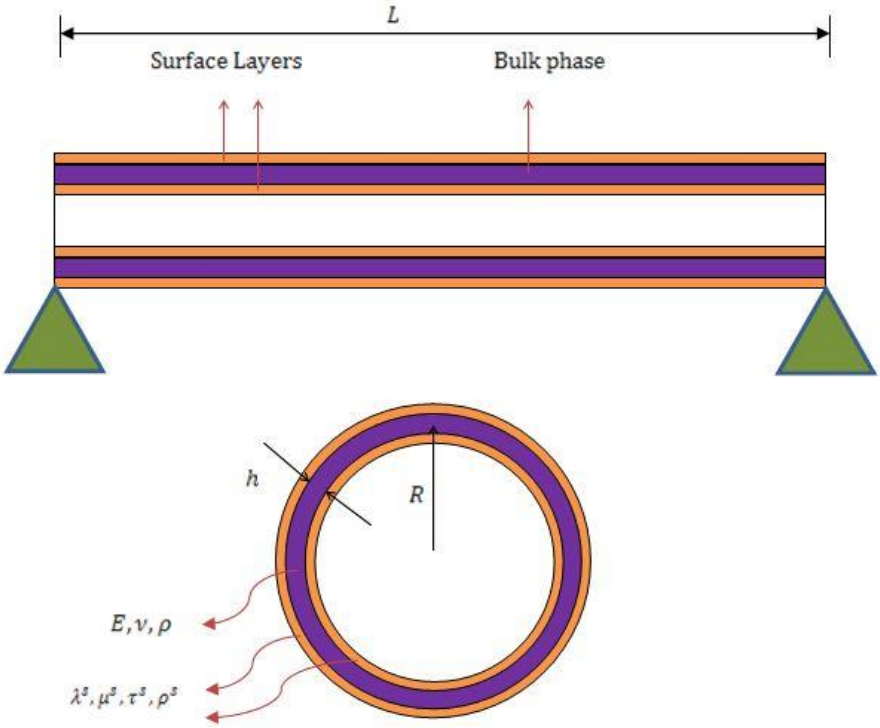

Fig. 1. Schematic view of a simply-supported cylindrical nanoshell with bulk and surface phases

The constitutive relations of the bulk part are also formulated as

$$\begin{Bmatrix}\sigma_{xx}\\ \sigma_{yy}\\ \sigma_{xy}\\ \sigma_{xz}\\ \sigma_{yz}\end{Bmatrix}=\begin{bmatrix}\lambda+2\mu & \lambda & 0 & 0 & 0\\ \lambda & \lambda+2\mu & 0 & 0 & 0\\ 0 & 0 & \mu & 0 & 0\\ 0 & 0 & 0 & \mu & 0\\ 0 & 0 & 0 & 0 & \mu\end{bmatrix}\begin{Bmatrix}\varepsilon_{xx}\\ \varepsilon_{yy}\\ \gamma_{xy}\\ \gamma_{xz}\\ \gamma_{yz}\end{Bmatrix} \quad (3)$$

where $\lambda = Ev/(1-v^2)$ and $\mu = E/(2(1+v))$ denote classical Lamé's parameters (E and v are Young's modulus and Poisson's ratio of bulk part, respectively).

Based on the Gurtin-Murdoch theory [31], the constitutive relation for the surface part is:

$$\begin{aligned}\sigma^s_{\alpha\beta} &= \tau^s\delta_{\alpha\beta}+(\tau^s+\lambda^s)\varepsilon^s_{\gamma\gamma}\delta_{\alpha\beta}+\\ &2(\mu^s-\tau^s)\varepsilon^s_{\alpha\beta}+\tau^s u^s_{\alpha,\beta} \qquad ;(\alpha,\beta=x,y)\\ \sigma^s_{\alpha z} &= \tau^s u^s_{z,\alpha}\end{aligned} \quad (4)$$

in which λ^s and μ^s are surface Lamé's parameters. Moreover, τ^s indicates the surface residual stress and $\delta_{\alpha\beta}$ denotes the Kronecker delta.

It should be remarked that using the Gurtin-Murdoch model (through the last term in its constitutive equation), it is possible to consider surface pre-strains developed on the surface before loading owing to the surface residual stress [42, 43]. Deformation of the surface before loading leads to large strains after loading. Therefore, by taking surface pre-strains into account, large strains are developed in the surface phase, whereas strains in the bulk phase are small [44].

Based on Equation (4), the surface stress components are obtained as:

$$\begin{aligned}&\sigma^s_{xx}=(\lambda^s+2\mu^s)\varepsilon^s_{xx}+(\tau^s+\lambda^s)\varepsilon^s_{yy}+\tau^s,\ \sigma^s_{xz}=\tau^s\frac{\partial w}{\partial x}\\ &\sigma^s_{yy}=(\lambda^s+2\mu^s)\varepsilon^s_{yy}+(\tau^s+\lambda^s)\varepsilon^s_{xx}-\tau^s\frac{w}{R}+\tau^s,\ \sigma^s_{yz}=\tau^s\frac{\partial w}{\partial y}\\ &\sigma^s_{xy}=\mu^s\gamma^s_{xy}-\tau^s\left(\frac{\partial v}{\partial x}+z\frac{\partial \psi_y}{\partial x}\right),\ \sigma^s_{yx}=\mu^s\gamma^s_{xy}-\tau^s\left(\frac{\partial u}{\partial y}+z\frac{\partial \psi_x}{\partial y}\right),\end{aligned} \quad (5)$$

In the context of classical continuum models, it is assumed that σ_{zz} is small as compared to other normal stresses, and hence it is neglected. But, such assumption does not satisfy the surface conditions of the present surface stress model. Therefore, it is considered that σ_{zz} changes linearly through the thickness and satisfies the equilibrium conditions on the surfaces [45]. If the surface stresses on the surfaces S^+ and S^- are denoted by $\sigma_{i\alpha}^{s+}$ and $\sigma_{i\alpha}^{s-}$, respectively, the following equilibrium relations must be satisfied [31].

$$\sigma_{\beta i,\beta}^{s+} - \sigma_{iz}^{s+} = \rho^{s+}\ddot{u}_i^{s+} \quad z = +h/2 \tag{6a}$$

$$\sigma_{\beta i,\beta}^{s-} + \sigma_{iz}^{s-} = \rho^{s-}\ddot{u}_i^{s-} \quad z = -h/2 \tag{6b}$$

where σ_{iz}^{s+} and σ_{iz}^{s-} are bulk stresses at $z = \pm h/2$, respectively, u_i^{s+} and u_i^{s-} are displacements at $z = \pm h/2$, respectively, and $\rho^{s\pm}$ are the surface densities of the surface layers S^+ and S^-, respectively.

Accordingly, σ_{zz} is written as:

$$\sigma_{zz} = \frac{\left(\frac{\partial \sigma_{xz}^{s+}}{\partial x} + \frac{\partial \sigma_{yz}^{s+}}{\partial y} - \rho^{s+}\frac{\partial^2 w}{\partial t^2}\right) - \left(\frac{\partial \sigma_{xz}^{s-}}{\partial x} + \frac{\partial \sigma_{yz}^{s-}}{\partial y} - \rho^{s-}\frac{\partial^2 w}{\partial t^2}\right)}{2} + \frac{\left(\frac{\partial \sigma_{xz}^{s+}}{\partial x} + \frac{\partial \sigma_{yz}^{s+}}{\partial y} - \rho^{s+}\frac{\partial^2 w}{\partial t^2}\right) + \left(\frac{\partial \sigma_{xz}^{s-}}{\partial x} + \frac{\partial \sigma_{yz}^{s-}}{\partial y} - \rho^{s-}\frac{\partial^2 w}{\partial t^2}\right)}{h} z \tag{7}$$

Using Equation (5) leads to

$$\sigma_{zz} = \frac{2z}{h}\left(\tau^s \frac{\partial^2 w}{\partial x^2} + \tau^s \frac{\partial^2 w}{\partial y^2} - \rho^s \frac{\partial^2 w}{\partial t^2}\right) \tag{8}$$

By substituting this relation into the relations of normal stresses for the bulk of the nanoshell one arrives at

$$\sigma_{xx} = (\lambda + 2\mu)\varepsilon_{xx} + \lambda\varepsilon_{yy} + \frac{\nu\sigma_{zz}}{(1-\nu)},$$
$$\sigma_{yy} = (\lambda + 2\mu)\varepsilon_{yy} + \lambda\varepsilon_{xx} + \frac{\nu\sigma_{zz}}{(1-\nu)}, \tag{9}$$

The total strain energy with considering the surface stress effect is expressed as

$$\Pi_s = \frac{1}{2}\int_S \int_{-\frac{h}{2}}^{\frac{h}{2}} \sigma_{ij}\varepsilon_{ij}\,dz\,dS + \frac{1}{2}\left(\int_{S^+} \sigma_{ij}^s \varepsilon_{ij}^s\,dS^+ + \int_{S^-} \sigma_{ij}^s \varepsilon_{ij}^s\,dS^-\right) =$$
$$\frac{1}{2}\int_S \left\{\bar{N}_{xx}\varepsilon_{xx}^0 + \bar{N}_{yy}\varepsilon_{yy}^0 + \bar{N}_{xy}\gamma_{xy}^0 + \bar{M}_{xx}\kappa_{xx} + \bar{M}_{yy}\kappa_{yy} + \bar{M}_{xy}\kappa_{xy} + Q_x\gamma_{xz} + Q_y\gamma_{yz} + Q_x^s\frac{\partial w}{\partial x} + Q_y^s\frac{\partial w}{\partial y}\right\} dS \tag{10}$$

where S is the area of middle plane. Furthermore, the in-plane force resultants, bending moments and shear forces are:

$$\bar{N}_{xx} = N_{xx} + \sigma_{xx}^{s+} + \sigma_{xx}^{s-} = A_{11}^*\varepsilon_{xx}^0 + A_{12}^*\varepsilon_{yy}^0 + 2\tau^s,$$
$$\bar{N}_{yy} = N_{yy} + \sigma_{yy}^{s+} + \sigma_{yy}^{s-} = A_{11}^*\varepsilon_{yy}^0 + A_{12}^*\varepsilon_{xx}^0 - \frac{2\tau^s w}{R} + 2\tau^s,$$
$$\bar{N}_{yy} = N_{yy} + \sigma_{yy}^{s+} + \sigma_{yy}^{s-} = A_{11}^*\varepsilon_{yy}^0 + A_{12}^*\varepsilon_{xx}^0 - \frac{2\tau^s w}{R} + 2\tau^s,$$
$$\bar{M}_{xx} = M_{xx} + \frac{h}{2}\left(\sigma_{xx}^{s+} - \sigma_{xx}^{s-}\right) = D_{11}^*\kappa_{xx} + D_{12}^*\kappa_{yy} + E_{11}^*\left(\frac{\partial^2 w}{\partial x^2} + \frac{\partial^2 w}{\partial y^2}\right) - G_{11}^*\frac{\partial^2 w}{\partial t^2},$$
$$\bar{M}_{yy} = M_{yy} + \frac{h}{2}\left(\sigma_{yy}^{s+} - \sigma_{yy}^{s-}\right) = D_{11}^*\kappa_{yy} + D_{12}^*\kappa_{xx} + E_{11}^*\left(\frac{\partial^2 w}{\partial x^2} + \frac{\partial^2 w}{\partial y^2}\right) - G_{11}^*\frac{\partial^2 w}{\partial t^2},$$
$$\bar{M}_{xy} = M_{xy} + \frac{h}{4}\left(\sigma_{xy}^{s+} + \sigma_{yx}^{s+} - \sigma_{xy}^{s-} - \sigma_{yx}^{s-}\right) = D_{55}^*\kappa_{xy}, \quad Q_x = k_s A_{55}\gamma_{xz}, \quad Q_y = k_s A_{55}\gamma_{yz},$$
$$Q_x^s = \sigma_{xz}^{s-} + \sigma_{xz}^{s+} = 2\tau^s\frac{\partial w}{\partial x}, \quad Q_y^s = \sigma_{yz}^{s-} + \sigma_{yz}^{s+} = 2\tau^s\frac{\partial w}{\partial y}. \tag{11}$$

in which

$$\begin{Bmatrix} N_{xx} \\ N_{yy} \\ N_{xy} \end{Bmatrix} = \int_{-\frac{h}{2}}^{\frac{h}{2}} \begin{Bmatrix} \sigma_{xx} \\ \sigma_{yy} \\ \sigma_{xy} \end{Bmatrix} dz, \begin{Bmatrix} M_{xx} \\ M_{yy} \\ M_{xy} \end{Bmatrix} = \int_{-\frac{h}{2}}^{\frac{h}{2}} \begin{Bmatrix} \sigma_{xx} \\ \sigma_{yy} \\ \sigma_{xy} \end{Bmatrix} z dz, \begin{Bmatrix} Q_x \\ Q_y \end{Bmatrix} = \kappa_s \int_{-\frac{h}{2}}^{\frac{h}{2}} \begin{Bmatrix} \sigma_{xz} \\ \sigma_{yz} \end{Bmatrix} dz \tag{12a}$$

$$A_{11}^* = (\lambda + 2\mu)h + 2(\lambda^s + 2\mu^s), \quad A_{12}^* = \lambda h + 2(\tau^s + \lambda^s), A_{55}^* = \mu h + 2\mu^s - \tau^s, A_{55} = \mu h,$$
$$D_{11}^* = \frac{(\lambda + 2\mu)h^3}{12} + \frac{(\lambda^s + 2\mu^s)h^2}{2}, \; D_{12}^* = \frac{\lambda h^3}{12} + \frac{(\tau^s + \lambda^s)h^2}{2}, \tag{12b}$$
$$E_{11}^* = \frac{\nu h^2 \tau^s}{6(1-\nu)}, \; D_{55}^* = \frac{\mu h^3}{12} + \frac{(2\mu^s - \tau^s)h^2}{4}, G_{11}^* = \frac{\rho^s \nu h^2}{6(1-\nu)}.$$

The kinetic energy is also formulated as

$$\Pi_T = \frac{1}{2}\int_S \left\{ I_0^* \left[\left(\frac{\partial u}{\partial t}\right)^2 + \left(\frac{\partial v}{\partial t}\right)^2 + \left(\frac{\partial w}{\partial t}\right)^2 \right] + I_1^* \left[\left(\frac{\partial \psi_x}{\partial t}\right)^2 + \left(\frac{\partial \psi_y}{\partial t}\right)^2 \right] \right\} dS \tag{13}$$

where

$$I_0^* = \rho h + 2\rho^s, \quad I_1^* = \frac{\rho h^3}{12} + \frac{\rho^s h^2}{2}. \tag{14}$$

In these equations, ρ and ρ^s are densities of bulk and surface parts, respectively. By applying Hamilton's principle ($\delta \int_{t_1}^{t_2} (\Pi_T - \Pi_s) dt = 0$), the governing equations can be derived as

$$\frac{\partial \bar{N}_{xx}}{\partial x} + \frac{\partial \bar{N}_{xy}}{\partial y} = I_0^* \frac{\partial^2 u}{\partial t^2}, \tag{15a}$$
$$\frac{\partial \bar{N}_{xy}}{\partial x} + \frac{\partial \bar{N}_{yy}}{\partial y} + \frac{Q_y}{R} = I_0^* \frac{\partial^2 v}{\partial t^2}, \tag{15b}$$
$$\frac{\partial (Q_x + Q_x^s)}{\partial x} + \frac{\partial (Q_y + Q_y^s)}{\partial y} - \frac{\bar{N}_{yy}}{R} = I_0^* \frac{\partial^2 w}{\partial t^2}, \tag{15c}$$
$$\frac{\partial \bar{M}_{xx}}{\partial x} + \frac{\partial \bar{M}_{xy}}{\partial y} - Q_x = I_1^* \frac{\partial^2 \psi_x}{\partial t^2}, \tag{15d}$$
$$\frac{\partial \bar{M}_{xy}}{\partial x} + \frac{\partial \bar{M}_{yy}}{\partial y} - Q_y = I_1^* \frac{\partial^2 \psi_y}{\partial t^2}, \tag{15e}$$

The boundary conditions are also obtained as

$$\delta u = 0 \quad or \; \bar{N}_{xx} n_x + \bar{N}_{xy} n_y = 0 \tag{16a}$$
$$\delta v = 0 \quad or \; \bar{N}_{xy} n_x + \bar{N}_{yy} n_y = 0 \tag{16b}$$
$$\delta w = 0 \; or \; \{Q_x + Q_x^s\} n_x + \{Q_y + Q_y^s\} n_y = 0, \tag{16c}$$
$$\delta \psi_x = 0 \; or \quad \bar{M}_{xx} n_x + \bar{M}_{xy} n_y = 0, \tag{16d}$$
$$\delta \psi_y = 0 \; or \quad \bar{M}_{xy} n_x + \bar{M}_{yy} n_y = 0. \tag{16e}$$

3. Solution Procedure

To embark on the solution of governing equations for the free vibration problem, the dimensionless form of equations is first obtained. To this end, the following dimensionless parameters are introduced

$$x \to xL, \quad y \to yR, \quad \{u, v, w\} \to \{u, v, w\} h, \quad \beta = \frac{L}{R}, \quad \tau = \frac{t}{L}\sqrt{A_{110}/I_{00}}, \quad \eta = \frac{L}{h},$$
$$\{a_{11}, a_{12}, a_{55}, T_s, a_{550}\} = \left\{ \frac{A_{11}^*}{A_{110}}, \frac{A_{12}^*}{A_{110}}, \frac{A_{55}^*}{A_{110}}, \frac{\tau^s}{A_{110}}, \frac{A_{55}}{A_{110}} \right\},$$
$$\{d_{11}, d_{12}, d_{55}, e_{11}\} = \left\{ \frac{A_{11}^*}{A_{110}h^2}, \frac{A_{12}^*}{A_{110}h^2}, \frac{A_{55}^*}{A_{110}h^2}, \frac{E_{11}^*}{A_{110}h^2} \right\}, \{I_0, I_2, g_{11}\} = \left\{ \frac{I_0^*}{I_{00}}, \frac{I_1^*}{I_{00}h^2}, \frac{G_{11}^*}{I_{00}h^2} \right\} \tag{17}$$

where $A_{110} = (\lambda + 2\mu)h$ and $I_{00} = \rho h$. By these parameters, the dimensionless form of Equation (15) becomes

$$a_{11}\frac{\partial^2 u}{\partial x^2}+a_{55}\beta^2\frac{\partial^2 u}{\partial y^2}+(a_{12}+a_{55})\beta\frac{\partial^2 v}{\partial y\,\partial x}+a_{12}\beta\frac{\partial w}{\partial x}=I_0\frac{\partial^2 u}{\partial \tau^2}, \tag{18a}$$

$$(a_{12}+a_{55})\beta\frac{\partial^2 u}{\partial y\,\partial x}+a_{11}\beta^2\frac{\partial^2 v}{\partial y^2}+a_{55}\frac{\partial^2 v}{\partial x^2}+a_{11}\beta^2\frac{\partial w}{\partial y}+k_s a_{550}\beta\left(\beta\frac{\partial w}{\partial y}+\eta\psi_y-\beta v\right)-2T^s\beta^2\frac{\partial w}{\partial y}=I_0\frac{\partial^2 v}{\partial t^2} \tag{18b}$$

$$k_s a_{550}\left(\eta\frac{\partial \psi_x}{\partial x}+\beta\eta\frac{\partial \psi_y}{\partial y}-\beta^2\frac{\partial v}{\partial y}\right)+\left(k_s a_{550}+2T^s\right)\left(\frac{\partial^2 w}{\partial x^2}+\beta^2\frac{\partial^2 w}{\partial y^2}\right)-a_{11}\beta^2\left(\frac{\partial v}{\partial y}+w\right)-a_{12}\beta\frac{\partial u}{\partial x}+2T^s\beta^2 w=I_0\frac{\partial^2 w}{\partial \tau^2}, \tag{18c}$$

$$d_{11}\frac{\partial^2 \psi_x}{\partial x^2}+d_{12}\beta\frac{\partial^2 \psi_y}{\partial y\,\partial x}+d_{55}\beta\left(\beta\frac{\partial^2 \psi_x}{\partial y^2}+\frac{\partial^2 \psi_y}{\partial y\,\partial x}\right)-k_s a_{550}\eta\left(\frac{\partial w}{\partial x}+\eta\psi_x\right)+\frac{e_{11}}{\eta}\left(\frac{\partial^3 w}{\partial x^3}+\beta^2\frac{\partial^3 w}{\partial x\,\partial y^2}\right)=I_1\frac{\partial^2 \psi_x}{\partial \tau^2}+\frac{g_{11}}{\eta}\frac{\partial^3 w}{\partial x\,\partial \tau^2}, \tag{18d}$$

$$d_{11}\beta^2\frac{\partial^2 \psi_y}{\partial y^2}+d_{55}\left(\beta\frac{\partial^2 \psi_x}{\partial y\,\partial x}+\frac{\partial^2 \psi_y}{\partial x^2}\right)+d_{12}\beta\frac{\partial^2 \psi_x}{\partial y\,\partial x}-k_s a_{550}\eta\left(\beta\frac{\partial w}{\partial y}+\eta\psi_y-\beta v\right)+\frac{e_{11}}{\eta}\left(\beta\frac{\partial^3 w}{\partial y\,\partial x^2}+\beta^3\frac{\partial^3 w}{\partial y^3}\right)=I_1\frac{\partial^2 \psi_y}{\partial \tau^2}+\frac{g_{11}\beta}{\eta}\frac{\partial^3 w}{\partial y\,\partial \tau^2}. \tag{18e}$$

A Navier-type solution method is used here to solve the free vibration problem. The simply-supported boundary conditions are expressed as

$$\bar{N}_{xx}=v=w=\bar{M}_{xx}=\psi_y=0 \tag{19}$$

The following displacement components satisfy both the governing equations given in Equation (18) and the boundary conditions given in Equation (19)

$$\begin{Bmatrix} u(t,x,y)\\ v(t,x,y)\\ w(t,x,y)\\ \psi_x(t,x,y)\\ \psi_y(t,x,y)\end{Bmatrix}=\sum_{m=1}^{\infty}\sum_{n=1}^{\infty}\begin{Bmatrix} \tilde{u}\cos(\alpha_n x)\sin(\beta_m y)\\ \tilde{v}\sin(\alpha_n x)\cos(\beta_m y)\\ \tilde{w}\sin(\alpha_n x)\sin(\beta_m y)\\ \tilde{\psi}_x\cos(\alpha_n x)\sin(\beta_m y)\\ \tilde{\psi}_y\sin(\alpha_n x)\cos(\beta_m y)\end{Bmatrix}e^{i\Omega\tau} \tag{20}$$

where $\alpha_n=n\pi$ and $\beta_m=m$ (n: the number of axial wavenumbers, m the number of circumferential wavenumbers). In addition, Ω is the dimensionless natural frequency. By substituting the displacement components into dimensionless governing equations, and then by eliminating the trigonometric functions, one can arrive at the following set of algebraic equations

$$\left\{\begin{bmatrix} K_{11} & K_{12} & K_{13} & 0 & 0\\ K_{21} & K_{22} & K_{23} & 0 & K_{25}\\ K_{31} & K_{32} & K_{33} & K_{34} & K_{35}\\ 0 & 0 & K_{43} & K_{44} & K_{44}\\ 0 & K_{52} & K_{53} & K_{54} & K_{54}\end{bmatrix}-\Omega^2\begin{bmatrix} I_0 & 0 & 0 & 0 & 0\\ 0 & I_0 & 0 & 0 & 0\\ 0 & 0 & I_0 & 0 & 0\\ 0 & 0 & 0 & I_1+g_{11}\alpha_n/\eta & 0\\ 0 & 0 & 0 & 0 & I_1+g_{11}\beta\beta_m/\eta\end{bmatrix}\right\}\mathbf{d}=0 \tag{21}$$

where $\mathbf{d}=\left[\tilde{u},\tilde{v},\tilde{w},\tilde{\psi}_x,\tilde{\psi}_y\right]^T$ and the coefficients $K_{ij}\,(i,j=1,\ldots,5)$ can be expressed as

$$\begin{aligned}
&K_{11}=-a_{11}\alpha_n^2-a_{55}\beta^2\beta_m^2, K_{12}=K_{21}=-(a_{12}+a_{55})\beta\alpha_n\beta_m, K_{13}=K_{31}=a_{12}\beta\alpha_n,\\
&K_{22}=-\alpha_n^2 a_{55}-\beta_m^2 a_{11}\beta^2-k_s a_{550}\beta^2, K_{23}=\left(a_{11}\beta^2+k_s a_{550}\beta^2-2T^s\beta^2\right)\beta_m,\\
&K_{25}=K_{52}=k_s a_{550}\beta\eta, K_{32}=(a_{11}+k_s a_{550})\beta^2\beta_m, K_{34}=-\alpha_n k_s a_{550}\eta,\\
&K_{35}=-k_s a_{550}\beta_m\beta\eta, K_{33}=-\left(\beta^2\beta_m^2+\alpha_n^2\right)\left(k_s a_{550}+2T^s\right)+\left(2T^s-a_{11}\right)\beta^2,\\
&K_{43}=-\alpha_n\left(k_s a_{550}\eta+e_{11}\left(\alpha_n^2+\beta^2\beta_m^2\right)/\eta\right), K_{53}=-\beta_m\beta\left(k_s a_{550}\eta+e_{11}\left(\alpha_n^2+\beta^2\beta_m^2\right)/\eta\right),\\
&K_{44}=-\alpha_n^2 d_{11}-\beta_m^2 d_{55}\beta^2-k_s a_{550}\eta^2,\ K_{45}=K_{54}=-\alpha_n\beta_m\beta\left(d_{12}+d_{55}\right),\\
&K_{55}=-\left(d_{55}\alpha_n^2+d_{11}\beta^2\beta_m^2+k_s a_{550}\eta^2\right).
\end{aligned} \tag{22}$$

Finally, by finding the eigenvalues of Equation (21) numerically, the natural frequencies of cylindrical nanoshell can be obtained.

4. Results and Discussion

First, two validation studies are performed to assure the accuracy of the developed shell model. Table 1 shows a comparison between the results of present work and those of [46] and [47] for vibrations of simply-supported shells based on the classical elasticity theory. In this table, the variation of fundamental frequency is presented with length-to-radius ratio. It is observed that an excellent agreement exists between the present results and the results of [46] and [47].

Moreover, in Table 2, a comparison is made between the results of present shell model with those of a beam model developed in [48] based on the surface elasticity theory. The results of this table are generated for simply-supported boundary conditions and also for various length-to-thickness ratios (L/R). It is observed that there is a good agreement between two sets of results.

In the following, selected numerical results are given to show the surface effects on the vibrational behavior of nanoshells. It is considered that the material of nanoshell is Si <100> whose properties are [49, 50]

$$E = 210\ GPa,\ \rho = 2331 kg/m^3,\ \nu = 0.24,$$
$$\lambda^s = -4.488\ N/m,\ \mu^s = -2.774\ N/m,$$
$$\tau^s = 0.605\ N/m,\ \rho^s = 3.17e-7\ kg/m^2$$

Figure 2 depicts the free vibration response of the nanoshell with different magnitudes of thickness predicted based on the surface stress model. Furthermore, the dimensionless results of classical model are presented in this figure. It is observed that as the thickness of nanoshell decreases, the dimensionless frequency increases due to surface stress effect. Also, one can see that the surface stress effect is more pronounced at small magnitudes of thickness, and the difference between the surface stress and classic results becomes insignificant for the sufficiently thick nanoshell. In other words, by decreasing the thickness of nanoshell, the energies of surface phase become considerable compared to those of bulk of material. But, with increasing the thickness of nanoshell, the energies of bulk phase increases, and thus the surface energies become insignificant.

Figues 3-6 show the effects of surface properties on the free vibration characteristics of the nanoshell. In Figure 3, the influence of surface residual tension can be studied. It is seen that when the surface residual tension increases, the nanoshell frequency becomes larger. Figures 4 and 5 also indicate the effects of surface Lamé's constants. As it can be seen, the free vibration response is dependent on both magnitude and sign of surface Lamé's constants especially for the nanoshell with small aspect ratios. Figures 4 and 5 reveal that the frequencies associated with the positive values of surface Lamé's constants are higher than the ones related to the negative values. The influence of surface mass density is also shown in Figure 6. It is observed that the frequency of the nanoshell tends to decrease by increasing ρ^s.

Table 1. Variation of fundamental frequencies (Hz) of simply-supported shell against length-to-radius ratio predicted by the present shell model and by the models of [46] and [47] based on the classical elasticity theory

($E = 205.098\,\text{GPa},\ \nu = 0.31,\ \rho = 8900\ \text{kg/m}^3,\ R = 1\,\text{m},\ \ h/R = 0.002$)

L/R	0.2	0.5	1	2	5
Present	417.4186	166.7423	82.9874	41.2155	16.0791
[46, 47]	417.54	166.76	82.993	41.217	16.079

Table 2. Comparison between the dimensionless frequencies calculated based on the present shell model and the ones reported in [48] based on the surface elasticity theory for different length-to-radius ratios ($h = 1\,\text{nm}, d/h = 5$)

L/R	Present surface stress shell model	Surface stress beam model [48]
45	0.2363	0.2341
90	0.2208	0.2204
135	0.2137	0.2126
200	0.2083	0.2076

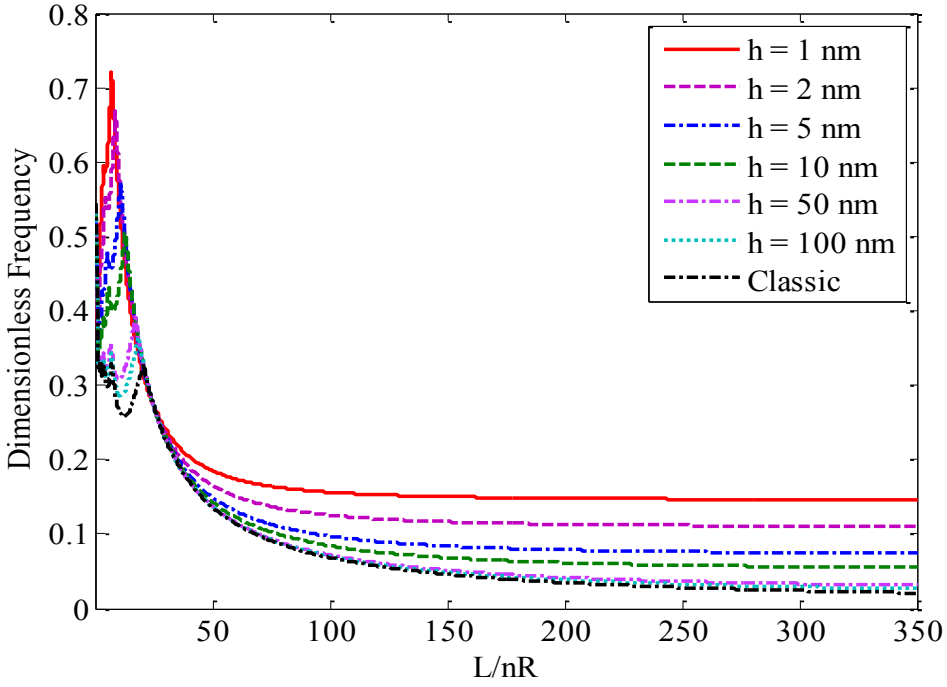

Fig. 2. Variation of dimensionless natural frequency with *L/nR* for different values of thickness (R/h=50)

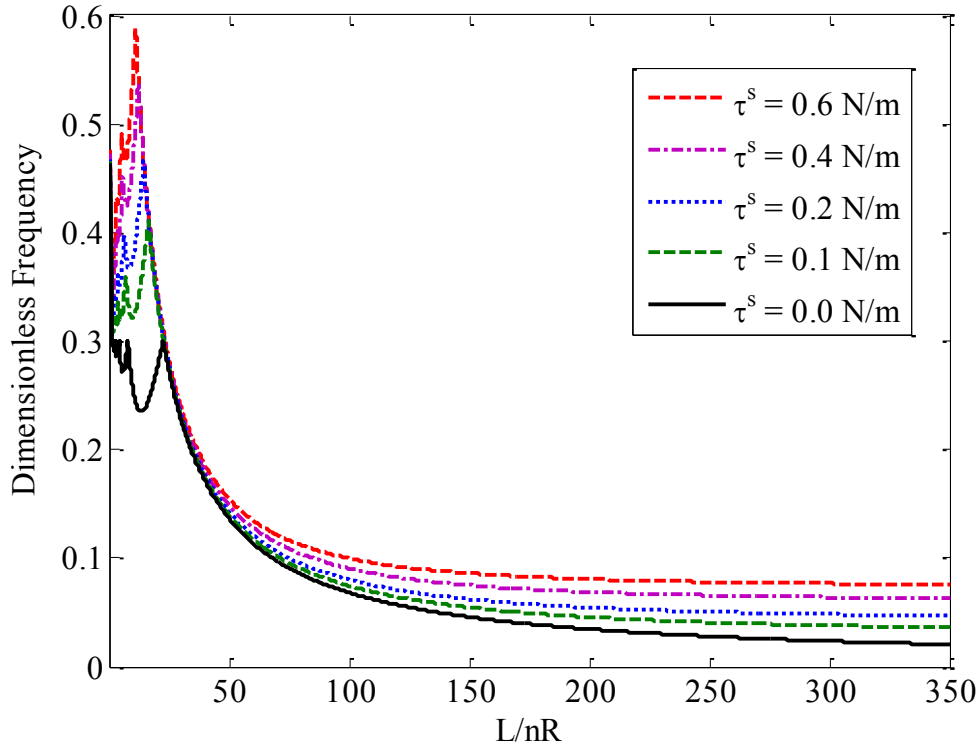

Fig. 3. Variation of dimensionless natural frequency with *L/nR* for different values of τ^s (R/h=60, h= 5nm)

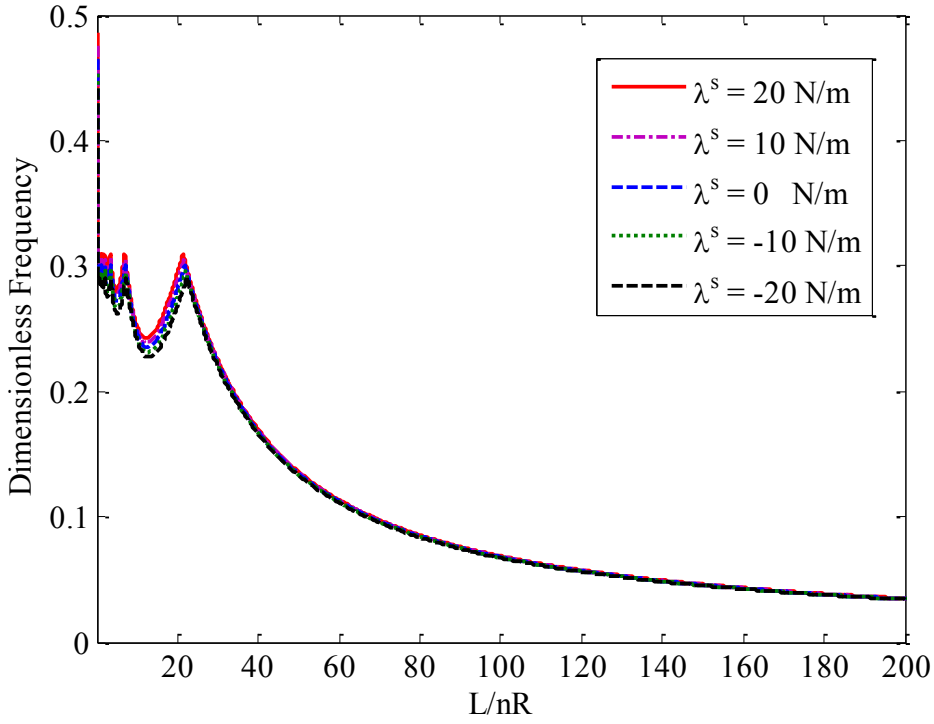

Fig. 4. Variation of dimensionless natural frequency with *L/nR* for different values of λ^s (R/h=60, h= 5nm)

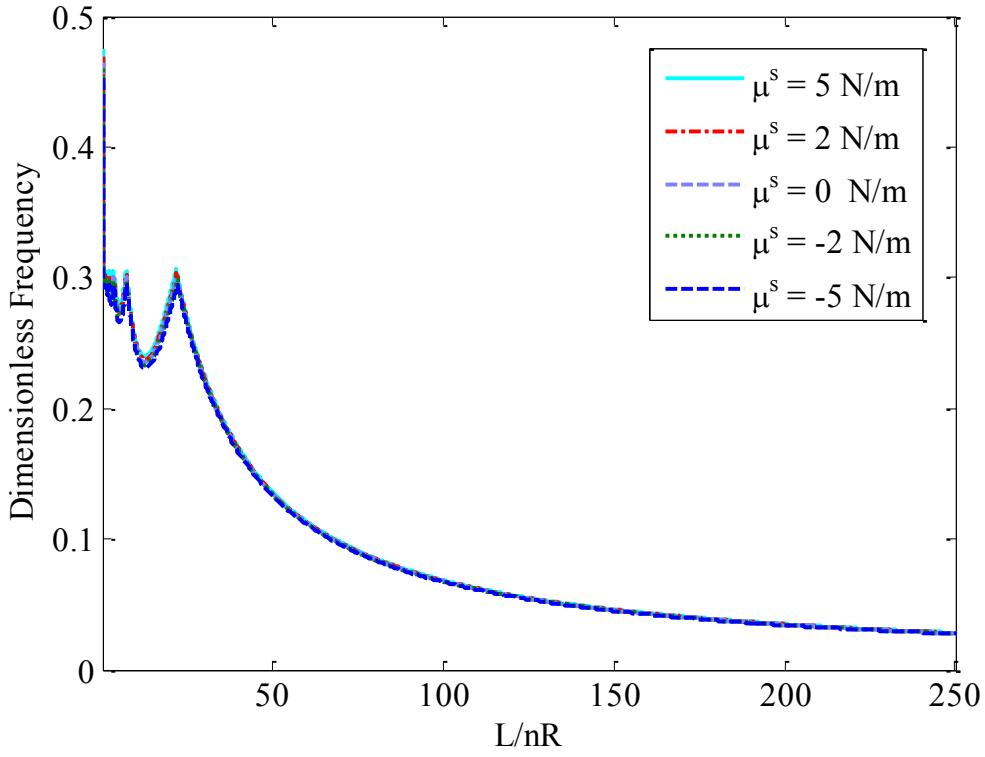

Fig. 5. Variation of dimensionless natural frequency with L/nR for different values of μ^s (R/h=60, h= 5nm)

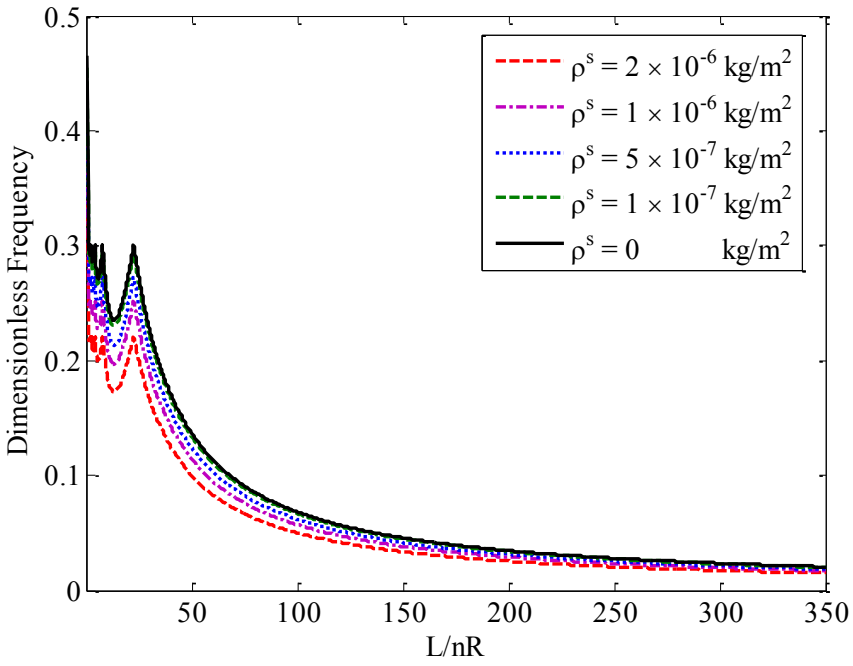

Fig. 6. Variation of dimensionless natural frequency with *L/nR* for different values of ρ^s (R/h=60, h= 5nm)

5. Conclusion

In this paper, the free vibration of nanoscale cylindrical shells was analyzed based on the Gurtin-Murdoch surface elasticity theory. The governing equations including surface stress effects were derived using Hamilton's principle. Then, in the case of the nanoshell under simply-supported end conditions, a closed-form solution was proposed. Selected numerical results were given to study the effects of surface stress on the vibrational behavior of the nanoshell. It was observed that the surface energies can significantly affect the free vibration of the nanoshell with small magnitudes of thickness. Moreover, it was indicated that the frequency of the nanoshell is dependent of the surface material properties.

References

[1]. Rafiee, M. A., Rafiee, J., Wang, Z., Song, H., Yu, Z. Z., and Koratkar, N., "Enhanced Mechanical Properties of Nanocomposites at Low Graphene Content," ACS Nano, Vol. 3, 2009, pp. 3884-3890.

[2]. Xia, Y., and Xiao, H., "Au Nanoplate/Polypyrrole Nanofiber Composite Film: Preparation, Characterization and Application as SERS Substrate," J. Raman Spectrosc., Vol. 43, 2012, pp. 469-473.

[3]. Abouzar, M. H., Poghossian, A., Pedraza, A. M., Gandhi, D., Ingebrandt, S., Moritz, W., and Schöning, M. J., "An Array of Field-Effect Nanoplate SOI Capacitors for (Bio-) Chemical Sensing," Biosens. Bioelec., Vol. 26, 2011, pp. 3023-3028.

[4]. Bi, L., Dong, J., Xie, W., Lu, W., Tong, W., Tao, L., and Qian, W., "Bimetallic Gold–Silver Nanoplate Array as a Highly Active SERS Substrate for Detection of Streptavidin/Biotin Assemblies," Anal. Chimica Acta, Vol. 805, 2013, pp. 95-100.

[5]. Khosroshahi, M. E., and Ghazanfari, L., "Synthesis of Three-Layered Magnetic Based Nanostructure for Clinical Application," Int. J. Nanosci. Nanotechnol., Vol. **7**, 2011, pp. 57-64.

[6]. Chang, S. T., and Hsieh, B. F., "TCAD Studies of Novel Nanoplate Amorphous Silicon Alloy Thin-Film Solar Cells," Thin Solid Films, Vol. 520, 2011, pp. 1612-1616.

[7]. Odom, T. W., Huang, J. L., Kim, P., Lieber, C. M., "Atomic Structure and Electronic Properties of Single-Walled Carbon Nanotubes," Nature, Vol. 391, 1998, 62–64.

[8]. Ganesan, Y., Peng, C., Lu, Y., Ci, L., Srivastava, A., Ajayan, P. M., and Lou, J., "Effect of Nitrogen Doping on the Mechanical Properties of Carbon Nanotubes," ACS Nano, Vol. 4, 2010, pp. 7637–7643.

[9]. Suk, J. W., Piner, R. D., An, J., and Ruoff, R. S., "Mechanical Properties of Monolayer Graphene Oxide," ACS Nano, Vol. 4, 2010, pp. 6557–6564.

[10]. Zakeri, M., and Shayanmehr, M., "On the Mechanical Properties of Chiral Carbon Nanotubes," J. Ultrafine Grained Nanostruct. Mater., Vol. 46, 2013, pp. 01-09.

[11]. Kumar, C. S. S. R., "Nanomaterials for Biosensors," Wiley-VCH, 2007, Wein-heim.

[12]. Zabow, G., Dodd, S. J., Moreland, J., and Koretsky, A. P., "The Fabrication of Uniform Cylindrical Nanoshells and Their Use as Spectrally Tunable MRI Contrast Agents," Nanotechnology, 20, 2009, 385301.

[13]. Zhu, J., Li, J. -J., and Zhao, J. -W., "Obtain Quadruple Intense Plasmonic Resonances from Multilayered Gold Nanoshells by Silver Coating: Application in Multiplex Sensing," Plasmonics, 8, 2013, 1493.

[14]. Yakobson, B. I., Brabec, C. J., and Bernholc, J., "Nanomechanics of Carbon Tubes: Instability Beyond Linear Response," Phys. Rev. Lett., Vol. 76, 1996, pp. 2511–2514.

[15]. Pantano, A., Boyce, M. C., and Parks, D. M., "Mechanics of Axial Compression of Single and Multi-Wall Carbon Nanotubes," ASME J. Eng. Mater. Technol., Vol. 126, 2004**,** pp. 279-284.

[16]. Yao, X., and Han, Q., "Buckling Analysis of Multiwalled Carbon Nanotubes Under Torsional Load Coupling With Temperature Change," ASME J. Eng. Mater. Technol., Vol. 128, 2006**,** pp. 419-427.

[17]. Ansari, R., Hemmatnezhad, M., and Ramezannezhad, H., "Application of HPM to the Nonlinear Vibrations of Multiwalled Carbon Nanotubes," Numer. Meth. Part. D. E. Vol. 26, 2009**,** pp. 490-500.

[18]. Mindlin, R. D., "Second Gradient of Strain and Surface Tension in Linear Elasticity," Int. J. Solids Struct., Vol. 1, 1965, pp. 417-438.

[19]. Lam, D. C. C., Yang, F., Chong, A. C. M., Wang, J., Tong, P., , "Experiments and Theory in Strain Gradient Elasticity," J. Mech. Phys. Solids, Vol. 51, 2003, pp. 1477-1508.

[20]. Ansari, R., Faghih Shojaei, M., Mohammadi, V., Gholami, R., and Rouhi, H., , "Nonlinear Vibration Analysis of Microscale Functionally Graded Timoshenko Beams Using the Most General Form of Strain Gradient Elasticity," J. Mech., Vol. 30, 2014, pp. 161-172.

[21]. Eringen, A. C., *Nonlocal Continuum Field Theories*, Springer, 2002, New York.

[22]. Prasanna Kumar, T. J., Narendar, S., Gupta, B. L. V. S., and Gopalakrishnan, S., "Thermal vibration analysis of double-layer graphene embedded in elastic medium based on nonlocal continuum mechanics," Int. J.Nano Dimens., Vol. 4, 2013, pp. 29-49.

[23]. Ansari, R., Faghih Shojaei, M., Shahabodini, A., and Bazdid-Vahdati, M., "Three-dimensional bending and vibration analysis of functionally graded nanoplates by a novel differential quadrature-based approach," Compos. Struct., Vol. 131, 2015, pp. 753-764.

[24]. Mindlin, R. D., and Tiersten, H. F., "Effects of Couple-Stresses in Linear Elasticity," Arch. Ration. Mech. Anal., Vol. 11, 1962, pp. 415-448.

[25]. Koiter, W. T., "Couple Stresses in the Theory of Elasticity," Proceedings of the Koninklijke Nederlandse Akademie van We tenschappen (B), Vol. 67, 1964, pp. 17-44.

[26]. Yang, F., Chong, A. C. M., Lam, D. C. C., and Tong, P., "Couple Stress Based Strain Gradient Theory for Elasticity," Int. J. Solids Struct., Vol. 39, 2002, pp. 2731-2743.

[27]. Shaat, M., "Effects of Grain Size and Microstructure Rigid Rotations on the Bending Behavior of Nanocrystalline Material Beams," Int. J. Mech. Sci., Vol. 94-95, 2015, pp. 27-35.

[28]. Shaat, M., and Abdelkefi, A., , "Modeling of Mechanical Resonators Used for Nanocrystalline Materials Characterization and Disease Diagnosis of HIVs," Microsyst. Technol., 2015, DOI 10.1007/s00542-015-2421-y.

[29]. Shaat, M., and Abdelkefi, A., "Modeling the Material Structure and Couple Stress Effects of Nanocrystalline Silicon Beams for Pull-In and Bio-Mass Sensing Applications," Int. J. Mech. Sci., Vol. 101-102, 2015, pp. 280-291.

[30]. Zhang, W. X., Wang, T. J., and Chen, X., "Effect of Surface/Interface Stress on the Plastic Deformation of Nanoporous Materials and Nanocomposites," Int. J. Plast., Vol. 26, 2010, pp. 957–975.

[31]. Gurtin, M. E., and Murdoch, A. I., "A Continuum Theory of Elastic Material Surface," Arch. Rat. Mech. Anal., Vol. 57, 1975, pp. 291-323.

[32]. Gurtin, M. E., and Murdoch, A. I., "Surface Stress in Solids," Int. J. Solids Struct., Vol. 14, 1978, pp. 431-440.

[33]. Chiu, M. S., and Chen, T., "Bending and Resonance Behavior of Nanowires Based on Timoshenko Beam Theory with High-Order Surface Stress Effects," Physica E, Vol. 54, 2013, pp. 149-156.

[34]. Shaat, M., Mahmoud, F. F., Gao, X. L., and Faheem, A. F., "Size-Dependent Bending Analysis of Kirchhoff Nano-Plates Based on a Modified Couple-Stress Theory Including Surface Effects," Int. J. Mech. Sci., Vol. 79, 2014, pp. 31-37.

[35]. Cheng, Ch. -H., and Chen, T., "Size-Dependent Resonance and Buckling Behavior of Nanoplates with High-Order Surface Stress Effects," Physica E, Vol. 67, 2015, pp. 12-17.

[36]. Ghorbanpour Arani, A., and Roudbari, M. A., "Surface Stress, Initial Stress and Knudsen-Dependent Flow Velocity Effects on the Electro-Thermo Nonlocal Wave Propagation of SWBNNTs," Physica B, Vol. 452, 2014, pp. 159-165.

[37]. Ansari, R., Ashrafi, M. A., Pourashraf, T., and Sahmani, S., "Vibration and Buckling Characteristics of Functionally Graded Nanoplates Subjected to Thermal Loading Based on Surface Elasticity Theory," Acta Astronautica, Vol. 109, 2015, pp. 42–51.

[38]. Ansari, R., Mohammadi, V., Faghih Shojaei, M., Gholami, R., and Sahmani, S., "Surface Stress Effect on the Postbuckling and Free Vibrations of Axisymmetric Circular Mindlin Nanoplates Subject to Various Edge Supports," Compos. Struct., Vol. 112, 2014, pp. 358-367.

[39]. Malekzadeh, P., and Shojaee, M., "Surface and Nonlocal Effects on the Nonlinear Free Vibration of Non-Uniform Nanobeams," Compos. Part B, Vol. 52, 2013, pp. 84-92.

[40]. Sharabiani, P. A., and Haeri Yazdi, M. R., "Nonlinear Free Vibrations of Functionally Graded Nanobeams with Surface Effects," Compos. Part B, Vol. 45, 2013, pp. 581-586.

[41]. Ansari, R., Mohammadi, V., Faghih Shojaei, M., Gholami, R., and Rouhi, H., "Nonlinear Vibration Analysis of Timoshenko Nanobeams Based on Surface Stress Elasticity Theory," Eur. J. Mech. A/Solids, Vol. 45, 2014, pp. 143-152.

[42]. Ru, C. Q., "Simple Geometrical Explanation of Gurtin-Murdoch Model of Surface Elasticity with Clarification of Its Related Versions," Sci. China Phys. Mech. Astron., Vol. 53, 2010, pp. 536–544.

[43]. Ru, C. Q., "A Strain-Consistent Elastic Plate Model with Surface Elasticity," Continuum Mech. Thermodyn, 2015., DOI 10.1007/s00161-015-0422-9.

[44]. Shaat, M., Eltaher, M. A., Gad, A. I., and Mahmoud, F. F., "Nonlinear Size-Dependent Finite Element Analysis of Functionally Graded Elastic Tiny-Bodies," Int. J. Mech. Sci., Vol. 77, 2013, pp. 356–364.

[45]. Lu, P., He, L. H., Lee, H. P., and Lu, C., "Thin plate theory including surface effects," Int. J. Solids Struct., Vol. 43, 2006, pp. 4631–4647.

[46]. Du, C., Li, Y., and Jin, X., "Nonlinear Forced Vibration of Functionally Graded Cylindrical Thin Shells," Thin-Walled Struct., Vol. 78, 2014, pp. 26–36.

[47]. Loy, C. T., Lam, K. Y., and Reddy, J. N., "Vibration of Functionally Graded Cylindrical Shells," Int. J. Mech. Sci., Vol. 41, 1999, pp. 309–324.

[48]. Ansari, R., Gholami, R., Norouzzadeh, A., and Darabi, M. A., "Surface Stress Effect on the Vibration and Instability of Nanoscale Pipes Conveying Fluid Based on a Size-Dependent Timoshenko Beam Model," Acta Mechanica Sinica, 31, 2015, pp. 708-719.

[49]. Zhu, R., Pan, E., Chung, P. W., Cai, X., Liew, K. M., and Buldum, A., "Atomistic Calculation of Elastic Moduli in Strained Silicon," Semicond. Sci. Technol., Vol. 21, 2006, pp. 906-911.

[50]. Miller, R. E., and Shenoy, V. B., "Size-Dependent Elastic Properties of Nanosized Structural Elements," Nanotechnology, Vol. 11, 2000, pp. 139-247.